Proc. Natl. Acad. Sci. USA
Vol. 86, pp. 307–311, January 1989
Medical Sciences

Lymphocyte antigen Leu-19 as a molecular marker of regeneration in human skeletal muscle

(immunofluorescence/laser scan microscopy/diseased human muscle/cultured myotubes/immunoprecipitation)

WALTER SCHUBERT*†‡, KATRIN ZIMMERMANN§, MATTHIAS CRAMER§, AND ANNA STARZINSKI-POWITZ§

*Neurologische Universitätsklinik, Sigmund Freud-Strasse 25, 5300 Bonn, Federal Republic of Germany; §Institut für Genetik, Universität zu Koeln, Weyertal 121, 5000 Koeln 41, Federal Republic of Germany; and ‡Zentrum für Molekulare Biologie der Universität Heidelberg, Im Neuenheimer Feld 282, 6900 Heidelberg, Federal Republic of Germany

Communicated by M. Lindauer, August 4, 1988 (received for review April 25, 1988)

ABSTRACT **Antigen Leu-19 (Leu19-Ag), a 200- to 220-kDa surface glycoprotein, was originally identified on a subset of human peripheral lymphocytes exhibiting non-major histocompatibility complex-restricted cytotoxicity. Here we report that monoclonal antibody Leu-19 (mAb-Leu19) labels structures in human skeletal muscle: (*i*) satellite cells, which form the stem cell pool of muscle fiber regeneration, both in normal and diseased muscle; (*ii*) myotubes and myotube projections in regions of muscle fiber repair; (*iii*) periodically organized fibrillar structures in areas of regeneration; (*iv*) the surface of myoblasts and developing myotubes in culture. mAb-Leu19 precipitated a protein of ≈200 kDa from cultured muscle cells. Our data show that Leu19-Ag is expressed on muscle-specific components of myosegments in repair and thus represents a molecular marker of muscle regeneration. On the basis of this molecular marker and using laser scan microscopy, it is possible to visualize at the light microscopic level hitherto undetectable details of muscle regeneration in routine cryostat sections.**

Segmental muscle fiber regeneration is a common phenomenon in disorders of human skeletal muscle, frequently leading to the reformation of a normal muscle fiber. Morphologically, the following stages of regeneration have been defined (1): (*i*) after local injury, retraction clots are formed on both sides of the injury; (*ii*) damaged segments between these contracted fiber ends undergo necrosis and are phagocytosed by macrophages; (*iii*) the satellite cells (SCs), which are the stem cells of regeneration and are located beneath the basal lamina of the muscle fiber, proliferate, migrate into the damaged region, and fuse to form myotubes. The latter may eventually fuse with the intact ends of the muscle fiber. The molecular signals that activate, direct, and arrange muscle repair are not yet established.

Muscle development in culture can be used as a tool to study structural and functional properties of stage-specific muscle proteins. Such proteins—e.g., the embryonic isoforms of myosin heavy chains—are also found in regenerating fibers of diseased muscle (2). Thus, myotube formation in culture can be a complementary system for studies of muscle regeneration *in situ*.

Using monoclonal antibody Leu-19 (mAb-Leu19), we identified a protein that is expressed on distinct structures confined to stage *iii* of regeneration and on developing muscle cells in culture. Antigen Leu-19 (Leu19-Ag) was originally characterized as a 200- to 220-kDa surface glycoprotein of human blood lymphocytes exhibiting non-major histocompatibility complex-restricted killing (3–5). Its function on lymphocytes is unknown.

Our immunohistological studies were performed by laser scan microscopy (6). This light microscopic technique has an optimized resolution that allows the rapid subcellular localization of weakly labeled small structures in routine cryostat sections such as that used in the present investigations. Thus, laser scan microscopy fills a need between conventional light and immune electron microscopy in medical and biological studies.

MATERIALS AND METHODS

Antibodies and Developing Reagents. *Primary reagents.* mAb-Leu19 antibody, phycoerythrin (PE) conjugated and unconjugated (Becton Dickinson); monoclonal anti-nuclear protein antibody 2A (mAb-NP; Paesel, Frankfurt); and monoclonal rat anti-laminin (mAb-lam) antibody (Dianova, Hamburg, F.R.G.) were used.

Secondary reagents. Texas red (TR)-labeled goat anti-mouse immunoglobulin (GaMIg) antibodies; unconjugated rabbit anti-mouse immunoglobulin antibodies; biotinylated goat $F(ab)_2$ antibodies to rat immunoglobulins (all Dianova); and unconjugated GaMIg (Ortho) were used.

Tertiary reagents. Streptavidin TR; peroxidase-conjugated mouse immunoglobulin (Amersham); and protein A-coupled Sepharose (Pharmacia) were used.

Incubations. Snap frozen skeletal muscle biopsies from patients with (*i*) limb-girdle muscular dystrophy (n = 3), (*ii*) polymyositis (n = 2), and (*iii*) spinal muscular atrophy (n = 4) were chosen for the immunohistological investigations. The morphological examination was made on cryostat sections that were stained with hematoxylin and eosin and trichrome and assayed for acid phosphatase and myofibrillary ATPase as described (7). The biopsy samples showed the typical morphological features of myopathy (*i*), inflammatory myopathy (*ii*), and neurogenic atrophy (*iii*). Furthermore, morphologically normal muscle from patients with internal disease (n = 2), who were tested because of conspicuous arteritis, were selected as controls. Cryostat sections (6 μm) were fixed in ice-cold acetone (10 min), air-dried, rehydrated in phosphate-buffered saline (PBS), and preincubated with normal goat serum (30 min, room temperature). For peroxidase-labelings, this was followed by mAb-Leu19 (PBS at 5 μg/ml), GaMIg, peroxidase-conjugated mouse immunoglobulin (30 min each), diaminobenzidine (5 μg/ml in 0.003% H_2O_2 for 10 min), and by counterstaining with hemalaun. For double-immunofluorescence studies sections were incubated first with mAb-lam (PBS at 2 μg/ml), second with biotinylated goat anti-rabbit or anti-rat immunoglobulin both followed by streptavidin TR, and finally by mAb-Leu19-PE (PBS at 5 μg/ml; 37°C; 20 min each). Sections were embed-

The publication costs of this article were defrayed in part by page charge payment. This article must therefore be hereby marked "*advertisement*" in accordance with 18 U.S.C. §1734 solely to indicate this fact.

Abbreviations: SC, satellite cell; mAb-Leu19, monoclonal antibody Leu-19; Leu19-Ag, antigen Leu-19; PE, phycoerythrin; mAb-NP, monoclonal anti-nuclear protein antibody 2A; mAb-lam, monoclonal rat anti-laminin antibody; TR, Texas red; GaMIg, goat anti-mouse immunoglobulin; N-CAM, neural cell adhesion molecule.

†To whom reprint requests should be addressed.

ded in Fluoromount (Southern Biotechnology, Birmingham, AL). For negative controls, nonimmune sera of mouse, rat, and rabbit were used instead of primary antibodies.

Immunofluorescence, Peroxidase Localizations, and Laser Scan Microscopy. In a first step, studies were done with a conventional microscope (Axiophot, Zeiss), equipped with epifluorescence optics, an HBO 50 vapor lamp, a video low light camera, and a B/W monitor. Fluorescence or peroxidase labelings were recorded on video tape for relocalizations within the same section and studies with the laser scan microscope (LSM 44; Zeiss) (8, 9). Details of laser scan microscopy will be published elsewhere. Fluorescence and phase-contrast images, generated by zoom magnifications from ×630 to ×10,000, were (*i*) recorded on video tape and (*ii*) photographed from the monitor either selectively or as transmitted light/incident light overlays in false color representation [PE (Leu-19), blue; TR, red; phase-contrast, green]. For precise colocalizations and correlation with morphology, coverslips were removed from sections, which were washed in PBS and counterstained with hematoxylin and eosin. Finally, the already recorded fields were relocalized in the laser scan microscope at the same magnifications and scanned as phase-contrast images.

Cells. Human skeletal myoblasts from a normal fetus (22 weeks of gestation) were grown and induced to myotube formation as described (10). For indirect immunofluorescence tests (10), cells were cultured on calf skin collagen-coated coverslips, stained with the first antibody in the presence of 0.1% sodium azide, fixed, incubated with GaMIg TR, and embedded in Fluoromount.

Immunoprecipitation. Cells were labeled with 100 μCi of [^{35}S]methionine (1 Ci = 37 GBq) per ml of cell culture medium for 4 hr, incubated with mAb-Leu19 in PBS with 0.1% sodium azide, washed, and lysed in 0.5% Nonidet P-40. Negative control dishes were incubated with mAb-NP instead of mAb-Leu19. After centrifugation (5 min, 14,000 × *g*), the antigen–antibody complexes were isolated from the supernatant with rabbit anti-mouse immunoglobulin antibodies absorbed to protein A-coupled Sepharose beads. Antigen-coated beads were washed and the bound antigen was analyzed on 7.5–15% denaturing and reducing polyacrylamide gradient gels (11), which were fluorographed.

RESULTS

Localization of Leu19-Ag on SCs. Cryostat sections of normal muscle were stained with mAb-Leu19 and developed either by the immunoperoxidase technique or by immunofluorescence as indicated (see *Materials and Methods*). At low magnification, immunoperoxidase reactions could hardly be detected in normal muscle (Fig. 1*a*). However, systematic screening of the sections at higher magnifications revealed specific staining with mAb-Leu19 of a small portion (10–20 cells per 16-mm^2 cross-section) of spindle-like structures closely attached to the muscle fiber surface (Figs. 2 and 3 *a–c*). These cellular structures were characterized as satellite cells by two criteria. First, they had spike-like projections (Fig. 2), which have never been found around myonuclei, and second, they were localized beneath the basal lamina (Fig. 3*b*). The latter was shown by double labelings with mAb-Leu19 and mAb-lam (Fig. 3 *a* and *b*). Laminin, recognized by mAb-lam, is a major protein of the basal lamina (12). The nonmacrophage and non-T-lymphocyte nature of these mononucleated cells was determined in 3-fold-labelings (8) using T-cell and macrophage markers [antibodies OKT8 (13) and OKM5 (14); unpublished observation]. In any case, macrophages have not been noted to express Leu19-Ag (3–5).

Localization of Leu19-Ag in Regenerating Fibers of Diseased Muscle. The subcellular localization of Leu19-Ag in normal muscle described above was extended to diseased muscle.

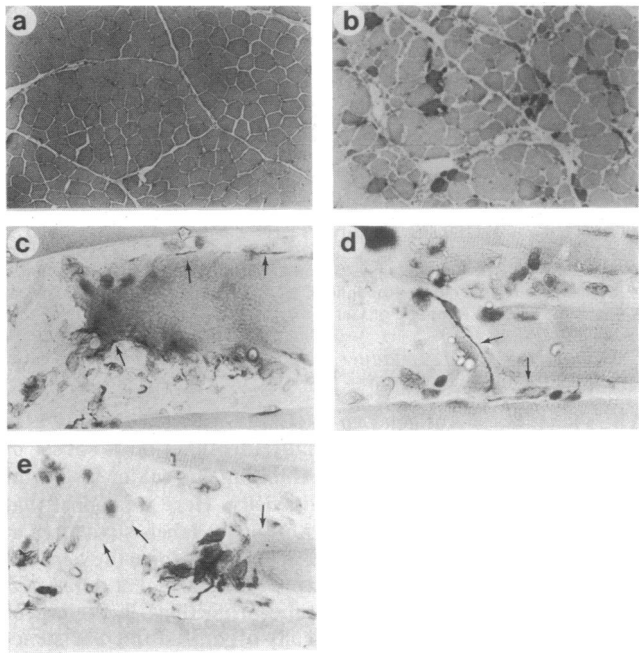

FIG. 1. Cryostat sections labeled with mAb-Leu19 (peroxidase, hemalaun counterstain). (*a* and *b*) Cross-sections of normal muscle (*a*) and polymyositis (*b*) (×100); (*c–e*) longitudinal sections of myopathic muscle. Leu-19$^+$ structures within damaged myosegments (×530); (*c*) contracted fiber end, which is bordered in part by Leu-19$^+$ structures (arrows); (*d*) single cell projection across damaged fiber area to another Leu-19$^+$ cell (arrows); (*e*) cell accumulation within the endomysial tube. Arrows mark intact fiber ends.

Skeletal muscle cryostat sections of myopathic (Figs. 1 *c–e*, 3 *d* and *e*, and 4), myositic (Figs. 1*b* and 5), and neurogenic syndromes (not shown) were stained with mAb-Leu19. We describe below the staining with mAb-Leu19 in sections of myopathic muscle. In longitudinal sections, defined stages of segmental muscle fiber alteration and repair could be identified within intact endomysial tubes: degeneration, phagocytosis, invasion, and fusion of mononuclear cells, most likely satellite cells, in empty endomysial tubes. As in normal muscle, Leu19-Ag was expressed on sublaminar satellite cells (Fig. 2), the number of which was apparently increased. Leu19-Ag was also found in regenerating areas of endomysial tubes (Fig. 1 *c–e*). Stages of muscle fiber repair have been defined morphologically (ref. 1; see Introduction and *Discussion*). When empty endomysial tubes could be seen, Leu19-Ag framed, in part, the zone of repair (Fig. 1*c*). In addition, at this stage of repair, single Leu-19$^+$ cells on opposite sides of the endomysial tube were connected by

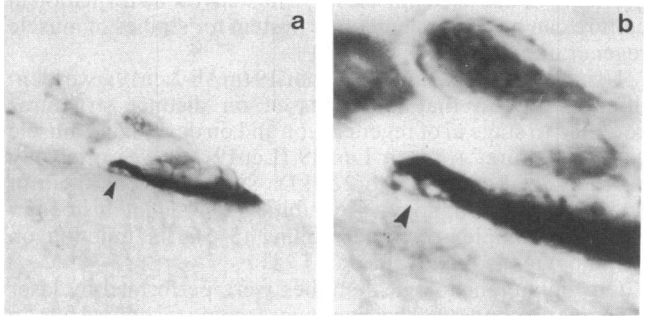

FIG. 2. Laser scan images of a Leu-19$^+$ cell most likely being a SC on the surface of a longitudinally sectioned muscle fiber (see also Fig. 3). (*a*, ×1450.) (*b*) Same cell, arrowhead to Leu-19$^+$ spike-like projections. (Zoom magnification, ×4410.)

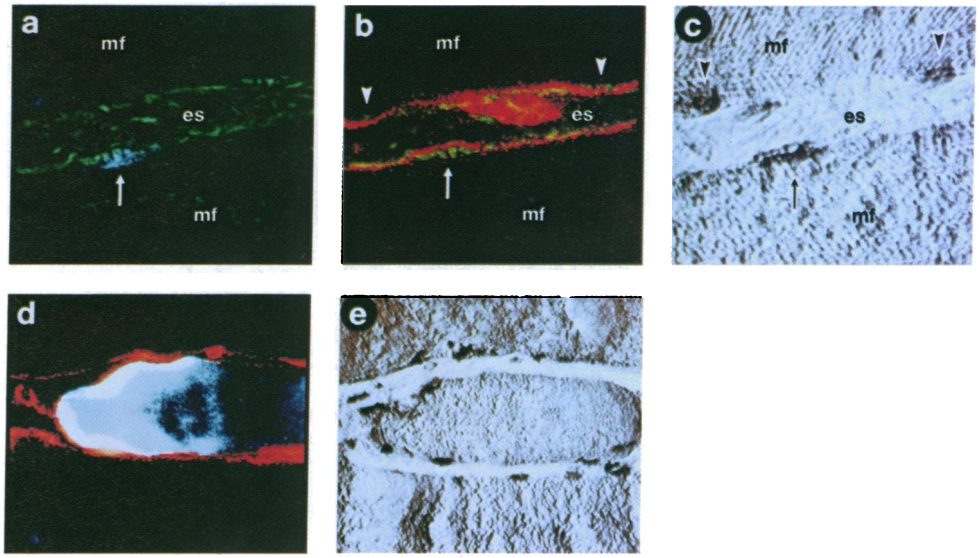

FIG. 3. Morphology-correlated laser scan microscopic images of double immunofluorescence in false color representation (longitudinal sections). (*a*) Leu-19$^+$ spindle-like SC (blue; arrow) in sublaminar position (*b*) (laminin: red). (*c*) Hematoxylin and eosin counterstain of the same section. mf, Muscle fiber; es, endomysial space. Note: Two Leu-19$^-$ sublaminar structures on the surface of the adjacent fiber (arrowheads in *b* and *c*) with a less dense chromatin than the Leu-19$^+$ cell. (*d*) Myopathy. Leu-19$^+$ muscle fiber (blue) surrounded by laminin-positive basal lamina (red). Change from dark to light blue represents increasing fluorescence intensity. (*e*) Hematoxylin and eosin counterstain of the same section. (*a–c*, ×2250; *d* and *e*, ×470.)

Leu-19$^+$ cellular projections (Fig. 1*d*). In a slightly later stage of regeneration, Leu19-Ag was also strongly expressed on clustering cells, which were most likely postmitotic SCs (Fig. 1*e*). In progressed stages of regeneration—i.e., cell fusion and filament formation—Leu19-Ag was detected on filamentous projections connecting the intact fiber regions neighboring the zone of repair (Fig. 4).

Details on these filaments could be studied with the laser scan microscope at high magnifications (×4600 to ×10,000) by scanning different focal planes in the zones of repair. Leu-19$^+$ labelings of filaments, which were projections of either myotubes (Fig. 4*a*) or tip formations of the remaining fiber ends (Fig. 4 *a* and *b*), were found. We interpreted the latter as muscle fiber growth cones. Periodic condensations were present at a distance of 2–2.5 μm (Fig. 4*c*). This corresponded to the mean periodicity of sarcomeres. The nodular condensations appeared to be anchors both of collateral branches of Leu-19$^+$ filament-like structures and of small Leu-19$^+$ loops (Fig. 4 *c* and *d*). Some loops seemed to be connected with neighboring loops of the collateral filament-like structure (Fig. 4*e*). Finally, myotubes and areas that appeared to be almost completely repaired showed Leu19-Ag expression in a cross-striational fashion, in particular within growth cones (Figs. 4 *a* and *b* and 5*a*). Overlay of Leu-19 fluorescence (Fig. 5*a*) with the corresponding phase-contrast image (Fig. 5*b*) in these areas showed that the Leu-19$^+$ labelings could be precisely projected on the thick filaments (overlay not shown). The results described above are presented schematically in a diagram (see Fig. 8; see also *Discussion*).

In addition to regenerating fibers in myopathy, Leu19-Ag was also found in neurogenic atrophic, polygonal hypertrophic, and some morphologically normal muscle fibers of the syndromes noted above. The latter observation may indicate the beginning and the end of regeneration processes in these morphologically unaltered fibers. Finally, expression of Leu-19 was not restricted to certain fiber types.

Expression of Leu19-Ag in Cultured Human Muscle Cells. To further substantiate the expression of Leu19-Ag in developing muscle cells, we (*i*) performed indirect immunofluorescence staining with mAb-Leu19 on both cultured human myotubes and myoblasts and (*ii*) immunoprecipitated the protein with mAb-Leu19 from biosynthetically labeled myotubes. In both techniques, mAb-Leu19 was incubated with living myotubes to check whether it is a surface protein. The indirect immunofluorescence staining revealed the presence of Leu19-Ag on the surface of cultured human myoblasts as well as on human myotubes developed in culture.

The patchy immunofluorescence staining appeared to be more intense in most of the myotubes (Fig. 6 *b* and *c*) when compared to myoblasts (Fig. 6*a*). Furthermore, the fluorescence staining with mAb-Leu19 was concentrated in certain areas of the myotubes and was also found on cell projections. In some cases, these projections connected two myotubes (Fig. 6 *b* and *c*). This finding was reminiscent of the projections seen in regenerating fibers *in situ* (Figs. 1*d* and 4).

Leu19-Ag has been shown to be a glycoprotein of 200–220 kDa in lymphocytes (3–5). We therefore carried out immunoprecipitation experiments with mAb-Leu19 by using [^{35}S]methionine-labeled cultured myotubes. The antigen–antibody complexes were isolated and analyzed in polyacrylamide gels (Fig. 7). Control dishes were incubated with mAb-NP, which should not react with living cells because it recognizes a nuclear antigen. mAb-Leu19 precipitated a protein of an apparent molecular mass of ≈200 kDa (Fig. 7). It was not possible to precipitate the Leu19-Ag from detergent lysates of cultured myotubes. This could mean that the Leu-19 epitope is unstable in solution. The immunoprecipitation experiment showed that muscle cells synthesize Leu19-Ag, which has a similar if not identical molecular mass in myotubes and peripheral lymphocytes.

DISCUSSION

In this paper, we have demonstrated the expression of a protein detected by mAb-Leu19 in normal and diseased adult human skeletal muscle and in cultured myoblasts and myotubes. This protein, which has a relative molecular mass of ≈200 kDa, is most likely the lymphocyte-typing antigen Leu-19.

Our results indicate that during morphological alterations, and independent of the underlying mechanisms, changes in the subcellular distribution pattern of Leu19-Ag do occur within the muscle fiber. The physiological expression of Leu19-Ag extends from SCs, which form the stem cell pool for muscle regeneration in normal muscle, to sites of regeneration in diseased fibers.

The morphological events of fiber repair, which follow the phagocytosis of degenerated muscle fiber segments, are (*i*) invasion of regional SCs into empty endomysial tubes, (*ii*) cell fusion, and (*iii*) reformation of the myofibrillar organization (1). It is essential for a correct remodeling of a damaged muscle fiber that proliferating SCs fuse with each other but not with mononuclear cells of other origin, like T cells or macrophages, which also invade the endomysial tube during regeneration. This selectivity of cell fusion in addition

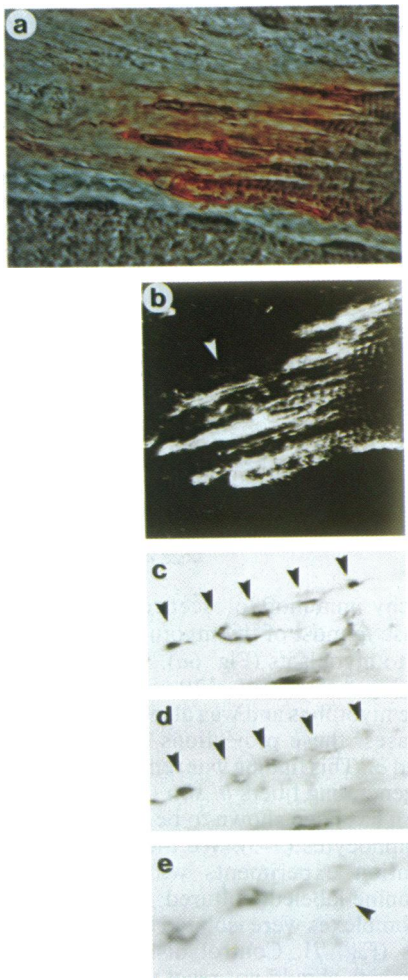

FIG. 4. Muscle fiber regeneration in a myopathy (longitudinal cryostat section labeled with peroxidase; hemalaun counterstain). (*a*) Zone of regeneration (phase contrast in conventional microscope). (×950.) (*b*) Selective demonstration of the peroxidase reaction of *a* in the laser scan microscope as negative monitor image. (×1060.) Note Leu-19$^+$ cross-striation in the growth cones. (*c–e*) Digitized laser scan images demonstrating high magnifications of Leu-19$^+$ filament-like structures (selectively scanned area is marked by arrowhead in *b*). Different focal planes show periodical arrangement of Leu-19$^+$ loops and condensations (distance of arrowheads, 2–2.5 μm). (*c* and *d*, ×3480.) (*e*) Magnification of structures in *d*. Some loops seem to fuse. (×7500.)

to correct longitudinal attachment of myotubes to intact fiber ends requires specific recognition molecules on both the cells to be fused and the structures to be repaired. Such molecules, which might be membrane proteins expressed upon activation, have not yet been established.

The staining pattern that we obtained with mAb-Leu19 is reminiscent of the neural cell adhesion molecule (N-CAM), which, among other things, participates in the formation of plexiform layers, neurite fasciculation, and nerve–muscle interactions (15, 16). In particular, N-CAM was, like Leu19-Ag, identified on SCs (17) and in cross-sections of regenerating muscle fibers of diseased muscle (18, 19). Despite these similarities, N-CAM has never been found on mammalian lymphocytes (ref. 21; C. Gondis, personal communication), and thus Leu19-Ag and N-CAM are likely to be distinct molecules.

Based on our results, we know that Leu19-Ag is at least a selective molecular marker of activated myogenic cells and regenerating structures. This might also suggest that Leu19-Ag is a functional component of a membrane recognition system in muscle regeneration.

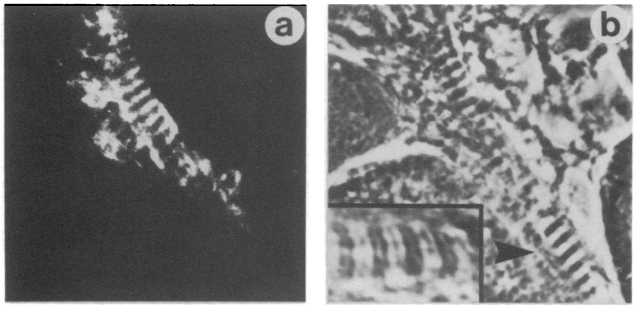

FIG. 5. Polymyositis (cryostat-section). Immunofluorescence of an incompletely differentiated and misoriented myotube in the laser scan microscope. (*a*) Leu19-Ag. (*b*) Phase contrast. A collateral branch of the myotube is shown (×1400.) Leu-19 is essentially expressed on the cell surface and on thick filaments. Note: lower part of the myotube, which shows complete sarcomere differentiation with clear I, A, Z, and H stripes (arrowhead; *Inset*), is unlabeled. (*Inset*) An oblique light laser scan image of the lower part of the myotube. The same technique revealed an undifferentiated sarcomere in the upper part.

The view of a selective marker molecule, presented schematically in Fig. 8, is supported by the following results and arguments.

(*i*) Spikes of SC and changes of their chromatin are thought to be signs of activation (1). We have shown that those cells are Leu-19$^+$ (Figs. 2 and 3 *a–c*). Leu19-Ag expression on SC may therefore indicate local muscle fiber deterioration. Low numbers of Leu-19$^+$ SCs in normal muscle could reflect physiological renewal of muscle fibers.

(*ii*) Leu19-Ag bordered partially contracted fiber ends (Fig. 1*c*) was found on myotube surfaces, and framed tip forma-

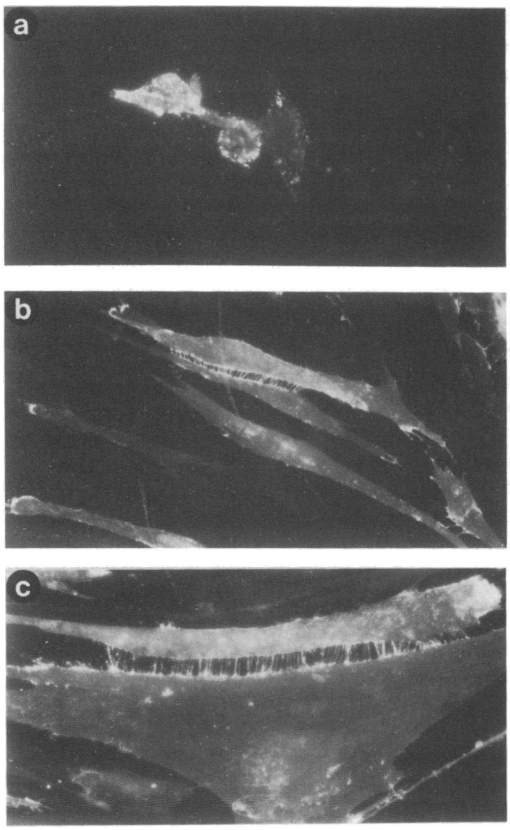

FIG. 6. Indirect TR immunofluorescence labeling with mAb-Leu19 on cultured human myoblasts (*a*) and myotubes (*b* and *c*). (×320.)

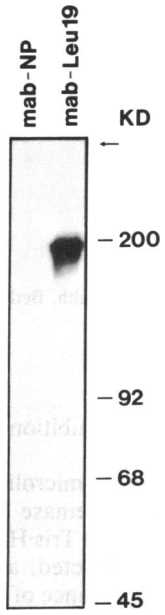

FIG. 7. Autoradiogram showing an immunoprecipitation experiment of protein Leu-19 from ^{35}S-labeled cultured human myotubes with mAb-Leu19. Negative control: mAb-NP recognizing a nuclear protein. Marker proteins: rainbow markers (Amersham). Gel was exposed for 3 days.

tions of the fiber ends, which we interpreted as growth cones. Myotubes were in part laterally connected if not fused with them (Fig. 4 *a* and *b*).

(*iii*) mAb-Leu19 labeled condensations at the sarcomere periodicity of 2.5 μm and loops on filament-like projections of myotubes and growth cones (Fig. 4 *c–e*). Similar projections were seen in cell culture (Fig. 6 *b* and *c*).

Interestingly, the periodical Leu-19$^+$ condensations on the filament-like structures (Fig. 4 *c* and *d*) resemble the dense bodies, which have been postulated to be the origin of myofibrillogenesis in chicken myocytes (20).

At present, we cannot show whether the synthesis of Leu19-Ag is really switched off when regeneration is completed. It is conceivable that Leu19-Ag is hidden in the mature intact muscle fiber and is thus undetectable by immunological methods.

Finally, we have found expression of Leu19-Ag in morphologically normal muscle fibers as mentioned in *Results*. This implies that the regenerative activity of muscle fibers can be detected with mAb-Leu19 at a time point when histological methods fail to detect damage let alone repair.

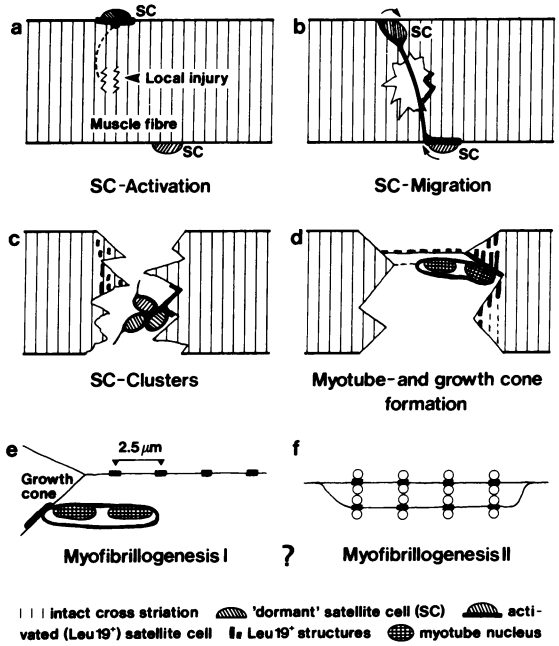

FIG. 8. Diagram of muscle fiber repair related to differential expression of protein Leu-19 and known stages of muscle repair (1). (*a*) Local injury of the muscle fiber and activation of local and dormant SCs. Signs of SC activation: Leu-19 on SCs (Figs. 2 and 3*a*); condensations of chromatin (Fig. 3*c*); development of Leu-19$^+$ spikes (Fig. 2). (*b*) SCs with Leu-19$^+$ projections across the damaged fiber area (Fig. 1*d*). (*c*) Leu-19$^+$ SCs assemble in the damaged area and stick to Leu-19$^+$ components of the endomysial tube (Fig. 1*e*). (*d–f*) Fusion of SCs to form myotubes. Leu-19$^+$ growth cones adhere to and fuse with Leu-19$^+$ myotubes. Myofibrillar reconstruction within the growth cones is accompanied by the expression of Leu19-Ag on the thick filaments (Fig. 4). Filament-like projections are sent across the repair zone from growth cones and myotubes. Leu-19$^+$ condensations and collateral fusing loops on these filaments occur strictly in the sarcomere periodicity and may be the precursors of Z lines and the scaffold for the sarcomere formation (myofibrillogenesis I and II; ref. 20).

Note Added in Proof. Surprisingly, Frank Walsh (University of London; personal communication) has found that mAb-Leu19 cross-reacts with mouse L cells that were transfected with the 140-kDa transmembrane form of human N-CAM cDNA. Whether this result is due to microheterogeneity of the N-CAM molecules expressed on different cell populations or to the serological properties of the antibody tested will be subject of further studies.

We wish to thank R. S. Jack and K. Beyreuther for critical reading of the manuscript, B. Müller-Hill for encouragement, G. Sticker and C. Schenkel for technical assistance, and U. Ringeisen for photographs. This work was supported by grants from the Deutsche Forschungsgemeinschaft (DFG Schu 627/1-1 and Sta 187/5-1, SFB 74/A5, 317/A8), the Bundesministerium für Forschung und Technologie, and the DECHEMA (fellowship to K.Z.).

1. Mazanet, R. & Franzini-Armstrong, C. (1986) in *Myology*, eds. Engel, A. G. & Banker, B. Q. (McGraw-Hill, New York), Vol. 1, pp. 285–307.
2. Webster, C., Silberstein, L., Hays, A. P. & Blau, H. M. (1988) *Cell* **52,** 503–513.
3. Griffin, J. D., Hercend, T., Beveredge, R. & Schlossmann, S. F. (1983) *J. Immunol.* **130,** 2947–2951.
4. Hercend, T., Griffin, J. D., Bensussan, A., Schmidt, R. E., Edson, M. A., Brennan, A., Murray, C. H., Daley, J. F., Schlossmann, S. F. & Ritz, J. (1985) *J. Clin. Invest.* **75,** 932–943.
5. Lanier, L. L., Le, A. M., Civin, C. J., Loken, M. R. & Phillips, J. H. (1986) *J. Immunol.* **136,** 4480–4486.
6. Wilke, V. (1985) *Scanning* **7,** 88–96.
7. Engel, A. G. (1986) in *Myology*, eds. Engel, A. G. & Banker, B. Q. (McGraw-Hill, New York), Vol. 1, pp. 833–843.
8. Schubert, W., Dominke, K. M. & Wilke, V. (1986) *Muscle Nerve* **9,** 248 (abstr.).
9. Schubert, W., Kontozis, L., Sticker, G., Schwan, H., Haraldsen, G. & Jerusalem, F. (1988) *Muscle Nerve* **11,** 890–892.
10. Zimmerman, K., Herget, T., Salbaum, J. M., Schubert, W., Hilbich, C., Cramer, M., Masters, C. L., Multhaup, G., Kang, J., Lemaire, H.-G., Beyreuther, K. & Starzinski-Powitz, A. (1988) *EMBO J.* **7,** 367–372.
11. Holtkamp, B., Cramer, M., Lemke, H. & Rajewsky, K. (1981) *Nature (London)* **289,** 66–68.
12. Sanes, J. R. (1982) *J. Cell Biol.* **93,** 442–451.
13. Reinherz, E. L., Kung, P. C., Goldstein, G. & Schlossmann, S. F. (1980) *J. Immunol.* **124,** 1301–1307.
14. Talle, M. A., Rao, P. E., Westberg, E., Allegar, N., Makowski, M., Mittler, R. S. & Goldstein, G. (1983) *Cell. Immunol.* **78,** 83–99.
15. Rutershauser, U. (1984) *Nature (London)* **310,** 549–554.
16. Edelman, G. M. (1986) *Annu. Rev. Physiol.* **48,** 417–430.
17. Covault, J. & Sanes, J. R. (1986) *J. Cell Biol.* **102,** 716–730.
18. Moore, S. E. & Walsh, F. S. (1985) *EMBO J.* **4,** 623–630.
19. Cashman, N. R., Covault, J., Wollmann, R. L. & Sanes, J. R. (1987) *Ann. Neurol.* **21,** 481–489.
20. Dlugosz, A. A., Antin, P. B., Machmias, V. T. & Holtzer, H. (1984) *J. Cell Biol.* **99,** 2266–2278.
21. Pierres, A., Naguet, P., van Agthoven, A., Bekkhoucha, F., Denizot, F., Mishal, Z., Schmitt-Verhulst, A.-M. & Pierres, M. (1984) *J. Immunol.* **132,** 2775–2782.